Motion Planning and Trajectory Control of an Underactuated Three-Link Robot via Dynamic Feedback Linearization*

Alessandro De Luca   Giuseppe Oriolo

Dipartimento di Informatica e Sistemistica
Università degli Studi di Roma "La Sapienza"
Via Eudossiana 18, 00184 Roma, Italy
{deluca,oriolo}@labrob.ing.uniroma1.it

Abstract

We present a new method for motion planning and feedback control of three-link planar robot arms with a passive rotational third joint. These underactuated mechanical systems are shown to be fully linearizable and input-output decoupable by means of a nonlinear dynamic feedback, provided a physical singularity is avoided. The linearizing output is the position of the so-called center of percussion of the third link. Based on this result, one can plan smooth motions joining in finite time any initial and desired final state of the robot. Moreover, it is easy to design an exponentially stabilizing feedback along the planned trajectory. Simulation results are reported for a 3R robot.

1 Introduction

A large effort has been devoted during the 90's to the dynamic analysis, motion planning, and feedback control of underactuated robots, i.e., second-order mechanical systems with less controls than degrees of freedom (see [1] and references therein).

Significant control analysis results can be found in [2] and [3]. Nonetheless, a general theory for planning and control of underactuated robots is not yet available and the most successful solutions were obtained tailoring the approach to the specific case considered. We limit the following review to ground-based rigid manipulators with passive joints (and no brakes).

The case of 2R planar robots under gravity with a single actuator has been considered in [4, 5] (Acrobot, passive first joint) and in [6] (Pendubot, passive second joint). The gravitational drift reduces the regions of the state space where these systems can be kept in equilibrium. Moving from one equilibrium manifold to another requires ad hoc appropriate swing-up maneuvers. However, since the approximate linearization of these robots is controllable, they are in principle relatively easy to control, at least locally.

The control of a planar 2R robot with an unactuated base joint in zero gravity is more intriguing. In [7] an oscillatory stabilizing feedback is designed for rest-to-rest motion tasks, based on a Poincaré map analysis. In [8], we have shown that the system fails to satisfy the weakest existing sufficient conditions for small-time local controllability (STLC), which implies that the design of feasible motion trajectories is an open problem. Moreover, smooth stabilization is not possible because the drift term tends to zero with the generalized velocities. The iterative state steering technique of [8], consisting of the repeated application of open-loop commands, guarantees the stabilization to a desired configuration. A numerical motion planner and a trajectory controller based on time-scaling has been proposed for the same system in [9].

The case of an underactuated three-link planar arm has been considered in [10], focusing on the rigid-body motion of the third link whose rotational joint is passive. This nonlinear system is proved to be STLC. Rest-to-rest motions are planned through a sequence of elementary maneuvers resembling those used for parking a wheeled mobile robot [11] or pushing a frictionless object [12]. In particular, they typically consist of a pure translation of the third link, followed by a pure rotation around its center of percussion (CP) and by another pure translation. Each maneuver starts and ends with zero velocity. If the initial and/or final states are not equilibria, two more deceleration/acceleration phases are needed. A different trajectory tracking controller is designed for each phase, so that a switching logic is necessary. On the other hand, in [13] it is shown that a planar PPR robot with a passive third joint can be transformed into a

*Work supported by MURST within the *RAMSETE* project.

second-order chained form via static feedback transformation. Two of the chained-form states are related to the coordinates of the CP.

In this paper, we build upon these works and exploit further the properties of the CP of the third link. Under the action of a second-order dynamic feedback compensator, the CP position (chosen as system output), together with its velocity, acceleration, and jerk, become an alternative set of state coordinates. The closed-loop system exhibits a fully linear and decoupled dynamics. Motion planning is then performed using smooth trajectories that interpolate, in a given finite time, any initial and desired final state. Trajectory tracking control is achieved using standard linear feedback techniques.

2 Three-link planar robot dynamics

The generic dynamic model of a three-link robot arm moving in a horizontal plane with a passive rotational third joint is

$$B(q)\ddot{q} + c(q,\dot{q}) = G(q)\begin{bmatrix}\tau_1\\ \tau_2\end{bmatrix}, \tag{1}$$

where $q = (q_1, q_2, q_3)$ is any set of generalized coordinates, and τ_1 and τ_2 are the available inputs on the first two joints. The 3×2 matrix $G(q)$ maps the inputs into generalized forces performing work on q.

We use a set of generalized coordinates that simplifies model analysis and control design, while capturing all the following cases of interest: RRR (3R), RPR, PRR, and PPR. Let $q = (x, y, \theta)$, where (x, y) are the cartesian coordinates of the base of the third link and θ is its orientation w.r.t. the x-axis. Letting $s\theta = \sin\theta$ and $c\theta = \cos\theta$, the dynamic model becomes

$$\left[\begin{array}{cc|c} \multicolumn{2}{c|}{B_a(x,y)} & \begin{array}{c}-m_3 d_3\, s\theta\\ m_3 d_3\, c\theta\end{array} \\ \hline -m_3 d_3\, s\theta & m_3 d_3\, c\theta & I_3 + m_3 d_3^2 \end{array}\right]\left[\begin{array}{c}\ddot{x}\\ \ddot{y}\\ \hline \ddot{\theta}\end{array}\right] + \left[\begin{array}{c} c_a(q,\dot{q}) \\ \hline 0\end{array}\right] = \left[\begin{array}{c}F_x\\ F_y\\ \hline 0\end{array}\right], \tag{2}$$

where I_3, m_3, and d_3 are, respectively, the baricentral inertia, mass, and distance of the center of mass from its base for the third link, and (F_x, F_y) are cartesian forces. Subscript a stands for actuated joints. Note that the third component of the Coriolis and centrifugal force vector vanishes.

2.1 Partial feedback linearization

To make the analysis independent from the nature of the first two joints, we perform first a partial linearization via static feedback of eq. (2). To this end, let

$$\begin{bmatrix}F_x\\ F_y\end{bmatrix} = c_a(q,\dot{q}) + \hat{B}_a(q)\begin{bmatrix}a_x\\ a_y\end{bmatrix},$$

where (a_x, a_y) are cartesian accelerations and matrix

$$\hat{B}_a(q) = B_a(x,y) - \frac{m_3 d_3^2}{I_3 + m_3 d_3^2}\begin{bmatrix} s^2\theta & -s\theta\, c\theta\\ -s\theta\, c\theta & c^2\theta\end{bmatrix}$$

is nonsingular being the Schur complement of diagonal element b_{33} of the positive definite inertia matrix B.

The resulting equations are similar to those used in [10] and [13]:

$$\begin{aligned} \ddot{x} &= a_x \\ \ddot{y} &= a_y \\ \ddot{\theta} &= \frac{1}{K}\,(\, s\theta\, a_x - c\theta\, a_y), \end{aligned} \tag{3}$$

where $K = (I_3 + m_3 d_3^2)/m_3 d_3$ is precisely the distance of the CP from the base of the third link. If uniform mass distribution is assumed for the third link, it is $K = 2\ell_3/3$ (ℓ_3 is the link length).

3 Linearization via dynamic feedback

We show below that system (3) can be transformed into a linear controllable system by means of nonlinear dynamic feedback and change of coordinates [14]. Define the CP cartesian position as the output:

$$\begin{bmatrix}y_1\\ y_2\end{bmatrix} = \begin{bmatrix}x\\ y\end{bmatrix} + K\begin{bmatrix}c\theta\\ s\theta\end{bmatrix}. \tag{4}$$

We apply the standard input-output decoupling algorithm, that involves differentiating the output until an auxiliary input appears in a nonsingular way. This may require the intermediate addition of integrators on the input channels, which become states of the dynamic compensator.

Differentiation of eq. (4) yields

$$\begin{bmatrix}\dot{y}_1\\ \dot{y}_2\end{bmatrix} = \begin{bmatrix}\dot{x}\\ \dot{y}\end{bmatrix} + K\dot{\theta}\begin{bmatrix}-s\theta\\ c\theta\end{bmatrix} \tag{5}$$

and

$$\begin{bmatrix}\ddot{y}_1\\ \ddot{y}_2\end{bmatrix} = \begin{bmatrix} c^2\theta & s\theta\, c\theta\\ s\theta\, c\theta & s^2\theta\end{bmatrix}\begin{bmatrix}a_x\\ a_y\end{bmatrix} - K\dot{\theta}^2\begin{bmatrix}c\theta\\ s\theta\end{bmatrix},$$

where eq. (3) has been used. Since the matrix multiplying the acceleration (a_x, a_y) is singular, we let

$$\begin{bmatrix}a_x\\ a_y\end{bmatrix} = \begin{bmatrix}c\theta & -s\theta\\ s\theta & c\theta\end{bmatrix}\begin{bmatrix}\xi\\ \alpha_2\end{bmatrix} = R(\theta)\begin{bmatrix}\xi\\ \alpha_2\end{bmatrix}, \tag{6}$$

and add an integrator on the (new) first input ξ

$$\dot{\xi} = \alpha_1'. \tag{7}$$

Vector (ξ, α_2) is the cartesian acceleration of the third link base, expressed in the moving frame attached to the link. As a result of (6), we have $\ddot{\theta} = -\alpha_2/K$ and

$$\begin{bmatrix} \ddot{y}_1 \\ \ddot{y}_2 \end{bmatrix} = (\xi - K\dot{\theta}^2) \begin{bmatrix} c\theta \\ s\theta \end{bmatrix}. \tag{8}$$

Using eqs. (3) and (7), the third derivative is

$$\begin{bmatrix} y_1^{[3]} \\ y_2^{[3]} \end{bmatrix} = \begin{bmatrix} c\theta & 2\dot{\theta}\, c\theta \\ s\theta & 2\dot{\theta}\, s\theta \end{bmatrix} \begin{bmatrix} \alpha_1' \\ \alpha_2 \end{bmatrix} + (\xi - K\dot{\theta}^2)\dot{\theta} \begin{bmatrix} -s\theta \\ c\theta \end{bmatrix}.$$

Since the input matrix is still singular, we perform a new input transformation

$$\begin{bmatrix} \alpha_1' \\ \alpha_2 \end{bmatrix} = \begin{bmatrix} 1 & -2\dot{\theta} \\ 0 & 1 \end{bmatrix} \begin{bmatrix} \eta \\ \alpha_2 \end{bmatrix}, \tag{9}$$

and add another integrator

$$\dot{\eta} = \alpha_1, \tag{10}$$

where η is dimensionally a jerk, obtaining

$$\begin{bmatrix} y_1^{[3]} \\ y_2^{[3]} \end{bmatrix} = R(\theta) \begin{bmatrix} \eta \\ (\xi - K\dot{\theta}^2)\dot{\theta} \end{bmatrix}. \tag{11}$$

Finally, the fourth derivative is computed as

$$\begin{bmatrix} y_1^{[4]} \\ y_2^{[4]} \end{bmatrix} = R(\theta) \begin{bmatrix} \alpha_1 + (K\dot{\theta}^2 - \xi)\dot{\theta}^2 \\ \dfrac{K\dot{\theta}^2 - \xi}{K}\, \alpha_2 + 2\eta\dot{\theta} \end{bmatrix}.$$

Under the regularity assumption $\gamma \triangleq \xi - K\dot{\theta}^2 \neq 0$, we apply inversion control

$$\begin{bmatrix} \alpha_1 \\ \alpha_2 \end{bmatrix} = \begin{bmatrix} 1 & 0 \\ 0 & \frac{K}{K\dot{\theta}^2 - \xi} \end{bmatrix} \left(R^T(\theta) \begin{bmatrix} v_1 \\ v_2 \end{bmatrix} - \begin{bmatrix} (K\dot{\theta}^2 - \xi)\,\dot{\theta}^2 \\ 2\eta\dot{\theta} \end{bmatrix} \right), \tag{12}$$

where (v_1, v_2) is the auxiliary input, giving

$$\begin{bmatrix} y_1^{[4]} \\ y_2^{[4]} \end{bmatrix} = \begin{bmatrix} v_1 \\ v_2 \end{bmatrix}, \tag{13}$$

i.e., two decoupled chains of four integrators.

Equation (13) represents the original system (3) under the action of the dynamic controller obtained combining eqs. (6–7) and (9–10) with the inversion controller (12). The sum of the differential orders (relative degrees) of the two outputs in eq. (13) is 8, equal to the dimension of the robot state plus the dimension of the compensator state $(\xi, \eta) \in I\!R^2$. Thus, full linearization is obtained [14].

The transformation from $(x, y, \theta, \dot{x}, \dot{y}, \dot{\theta}, \xi, \eta)$ to the linearizing coordinates $(y_1, y_2, \dot{y}_1, \dot{y}_2, \ldots, y_1^{[3]}, y_2^{[3]})$ is given by eqs. (4–5), (8) and (11). The inverse map from the solutions of eq. (13) to the robot and compensator states is:

$$\begin{aligned}
\theta &= \mathrm{ATAN2}\,\{\mathrm{sign}(\gamma)\ddot{y}_2, \mathrm{sign}(\gamma)\ddot{y}_1\} \\
\dot{\theta} &= \frac{c\theta\, y_2^{[3]} - s\theta\, y_1^{[3]}}{s\theta\, \ddot{y}_2 + c\theta\, \ddot{y}_1} \\
\xi &= c\theta\, \ddot{y}_1 + s\theta\, \ddot{y}_2 + K\dot{\theta}^2 \\
\eta &= c\theta\, y_1^{[3]} + s\theta\, y_2^{[3]} \\
\begin{bmatrix} x \\ y \end{bmatrix} &= \begin{bmatrix} y_1 \\ y_2 \end{bmatrix} - K \begin{bmatrix} c\theta \\ s\theta \end{bmatrix} \\
\begin{bmatrix} \dot{x} \\ \dot{y} \end{bmatrix} &= \begin{bmatrix} \dot{y}_1 \\ \dot{y}_2 \end{bmatrix} - K\dot{\theta} \begin{bmatrix} -s\theta \\ c\theta \end{bmatrix}.
\end{aligned}$$

The inverse transformation is regular iff $\gamma \neq 0$. From eq. (8), we note that $\gamma^2 = \ddot{y}_1^2 + \ddot{y}_2^2$, and thus the regularity condition can be checked before actually computing $\dot{\theta}$ and ξ. Physically, $\gamma \neq 0$ means that the linear acceleration ξ of the third-link base along the link axis should not be due *only* to an instantaneous rotation around the CP, which produces the centrifugal acceleration $K\dot{\theta}^2$. Thus, a pure rotation around the CP is the only motion not admissible with this linearization scheme.

4 Motion planning

Planning a feasible motion on the equivalent representation (13) can be formulated as an interpolation problem using smooth parametric functions $y_1(s)$ and $y_2(s)$, with a timing law $s = s(t)$. For simplicity, we directly generate trajectories $y_1(t)$ and $y_2(t)$.

At time $t = 0$, the robot starts from a generic state $(x_s, y_s, \theta_s, \dot{x}_s, \dot{y}_s, \dot{\theta}_s)$ and should reach, at $t = T$, a goal state $(x_g, y_g, \theta_g, \dot{x}_g, \dot{y}_g, \dot{\theta}_g)$. To obtain the boundary conditions for $y_1(t)$, $y_2(t)$ and their derivatives, we use eqs. (4–5), (8) and (11), where $\xi(0) = \xi_s$, $\xi(T) = \xi_g$, $\eta(0) = \eta_s$, and $\eta(T) = \eta_g$ can be chosen arbitrarily.

As an example, for a rest-to-rest motion ($\dot{x}_s = \dot{y}_s = \dot{\theta}_s = \dot{x}_g = \dot{y}_g = \dot{\theta}_g = 0$), we have for the first output

$$\begin{bmatrix} y_{1s} \\ \dot{y}_{1s} \\ \ddot{y}_{1s} \\ y_{1s}^{[3]} \end{bmatrix} = \begin{bmatrix} x_s + K\, c\theta_s \\ 0 \\ \xi_s\, c\theta_s \\ \eta_s\, c\theta_s \end{bmatrix}, \quad \begin{bmatrix} y_{1g} \\ \dot{y}_{1g} \\ \ddot{y}_{1g} \\ y_{1g}^{[3]} \end{bmatrix} = \begin{bmatrix} x_g + K\, c\theta_g \\ 0 \\ \xi_g\, c\theta_g \\ \eta_g\, c\theta_g \end{bmatrix},$$

and for the second output

$$\begin{bmatrix} y_{2s} \\ \dot{y}_{2s} \\ \ddot{y}_{2s} \\ y_{2s}^{[3]} \end{bmatrix} = \begin{bmatrix} y_s + K\, s\theta_s \\ 0 \\ \xi_s\, s\theta_s \\ \eta_s\, s\theta_s \end{bmatrix}, \quad \begin{bmatrix} y_{2g} \\ \dot{y}_{2g} \\ \ddot{y}_{2g} \\ y_{2g}^{[3]} \end{bmatrix} = \begin{bmatrix} y_g + K\, s\theta_g \\ 0 \\ \xi_g\, s\theta_g \\ \eta_g\, s\theta_g \end{bmatrix}.$$

A straightforward solution to this interpolation problem is to use polynomials of seventh degree:

$$y_i(t) = \sum_{j=1}^{7} a_{ij}\lambda^j, \qquad i = 1, 2,$$

with normalized time $\lambda = t/T$. The open-loop commands to system (13) are ($i = 1, 2$):

$$v_i(t) = \frac{1}{T^4}\left(840 a_{i7}\lambda^3 + 360 a_{i6}\lambda^2 + 120 a_{i5}\lambda + 24 a_{i4}\right).$$

Dropping the output index i, the expressions of the coefficients a_j are:

$$\begin{aligned}
a_0 &= y_s \\
a_1 &= \dot{y}_s T \\
a_2 &= \tfrac{1}{2}\ddot{y}_s T^2 \\
a_3 &= \tfrac{1}{6} y_s^{[3]} T^3 \\
a_4 &= 35(y_g - y_s) - (20\dot{y}_s + 15\dot{y}_g)T - (5\ddot{y}_s - \tfrac{5}{2}\ddot{y}_g)T^2 - (\tfrac{2}{3} y_s^{[3]} + \tfrac{1}{6} y_g^{[3]})T^3 \\
a_5 &= -84(y_g - y_s) + (45\dot{y}_s + 39\dot{y}_g)T + (10\ddot{y}_s - 7\ddot{y}_g)T^2 + (y_s^{[3]} + \tfrac{1}{2} y_g^{[3]})T^3 \\
a_6 &= 70(y_g - y_s) - (36\dot{y}_s + 34\dot{y}_g)T - (\tfrac{15}{2}\ddot{y}_s - \tfrac{13}{2}\ddot{y}_g)T^2 - (\tfrac{2}{3} y_s^{[3]} + \tfrac{1}{2} y_g^{[3]})T^3 \\
a_7 &= -20(y_g - y_s) + 10(\dot{y}_s + \dot{y}_g)T + 2(\ddot{y}_s - \ddot{y}_g)T^2 + \tfrac{1}{6}(y_s^{[3]} + y_g^{[3]})T^3.
\end{aligned}$$

The selection of initial and final compensator states (ξ_s, η_s) and (ξ_g, η_g) affects the boundary conditions, and thus the generated motion inside the chosen class of interpolating functions. In the rest-to-rest case, ξ_s and ξ_g should be nonzero and of the same sign, in order to avoid the singularity $\gamma = 0$ during the motion. In particular, if a pure translation of the third link is desired, the task can be split in two natural phases (say, acceleration and deceleration) so that ξ can be reset (changing its sign) at the intermediate time. This possibility of (re)initializing both ξ and η allows in general to avoid singularities.

To illustrate the performance of the planner, we present two typical results obtained for $T = 10$ s, $K = 2/3$ ($\ell_3 = 1$ m), and $\eta_s = \eta_g = 0$.

Figures 1–5 refer to the rest-to-rest planning

$$\begin{bmatrix} x_s \\ y_s \\ \theta_s \end{bmatrix} = \begin{bmatrix} 0.5\,\text{m} \\ 1\,\text{m} \\ 0^\circ \end{bmatrix} \longrightarrow \begin{bmatrix} x_g \\ y_g \\ \theta_g \end{bmatrix} = \begin{bmatrix} 1.5\,\text{m} \\ 2\,\text{m} \\ 45^\circ \end{bmatrix},$$

with $\xi_s = \xi_g = -0.1$ m/s^2. The time evolution of the CP position is shown in Fig. 1, while the cartesian motion of the third link is given in Fig. 2. The motion of a complete 3R arm (with $\ell_1 = \ell_2 = 1.5$ m), obtained by kinematic inversion, is given in Fig. 3, while the relative joint angles $\theta(t)$ are shown in Fig. 4. The nominal torques in Fig. 5 are obtained from the inverse dynamics (1) with the following mass data (links are thin rods of uniform mass): $m_1 = 10$, $m_2 = 5$, $m_3 = 1$ (kg).

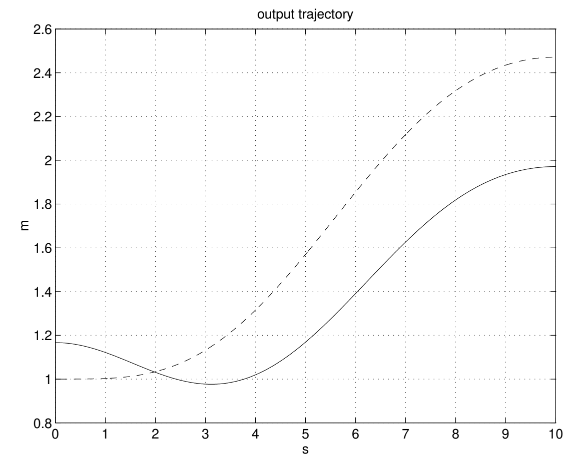

Figure 1: Rest-to-rest planning: y_1 (—), y_2 (−−)

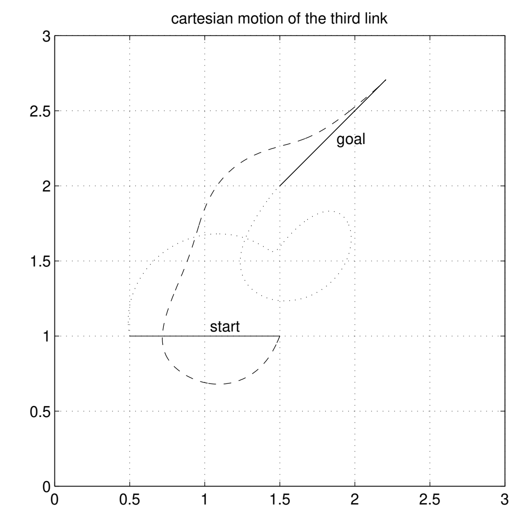

Figure 2: Rest-to-rest planning: Third link motion

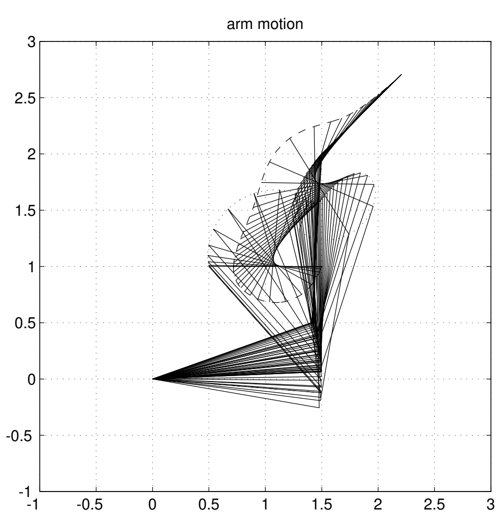

Figure 3: Rest-to-rest planning: 3R arm motion

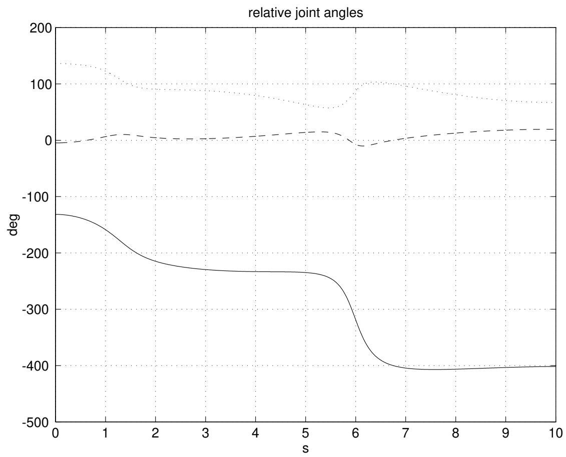

Figure 4: Rest-to-rest planning: θ_1 $(\cdots)$, θ_2 $(--)$ and θ_3 (—)

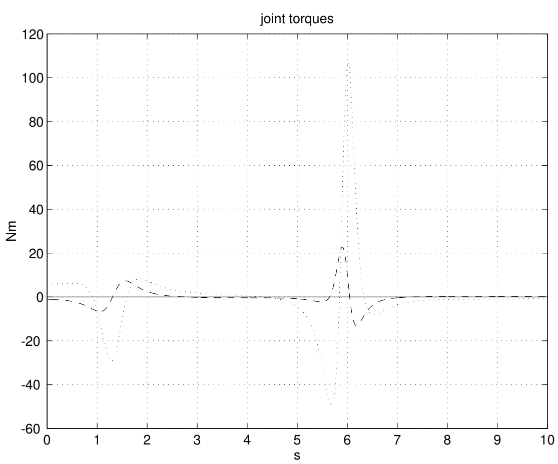

Figure 5: Rest-to-rest planning: τ_1 $(\cdots)$, τ_2 $(--)$

Note the high joint velocities and peak torques around $t = 6$ s, corresponding to a rapid rotation of the third link approximately around its CP — and thus to a decrease of the singularity index γ.

In Figs. 6–9 we report the results for the motion-to-rest planning

$$\begin{bmatrix} x_s \\ y_s \\ \theta_s \\ \dot{x}_s \\ \dot{y}_s \\ \dot{\theta}_s \end{bmatrix} = \begin{bmatrix} 1\,\mathrm{m} \\ 1\,\mathrm{m} \\ 0^\circ \\ -0.1\,\mathrm{m/s} \\ -0.1\,\mathrm{m/s} \\ 30^\circ/\mathrm{s} \end{bmatrix} \longrightarrow \begin{bmatrix} x_g \\ y_g \\ \theta_g \\ \dot{x}_g \\ \dot{y}_g \\ \dot{\theta}_g \end{bmatrix} = \begin{bmatrix} 1\,\mathrm{m} \\ 1\,\mathrm{m} \\ 90^\circ \\ 0\,\mathrm{m/s} \\ 0\,\mathrm{m/s} \\ 0^\circ/\mathrm{s} \end{bmatrix},$$

with $\xi_s = \xi_g = -0.1$ m/s^2. The joint velocities $\dot{\theta}(t)$ smoothly go to zero, without the need of an extra deceleration phase.

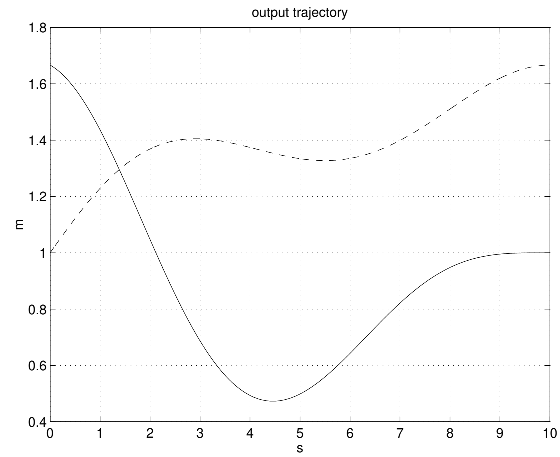

Figure 6: Motion-to-rest planning: y_1 (—), y_2 $(--)$

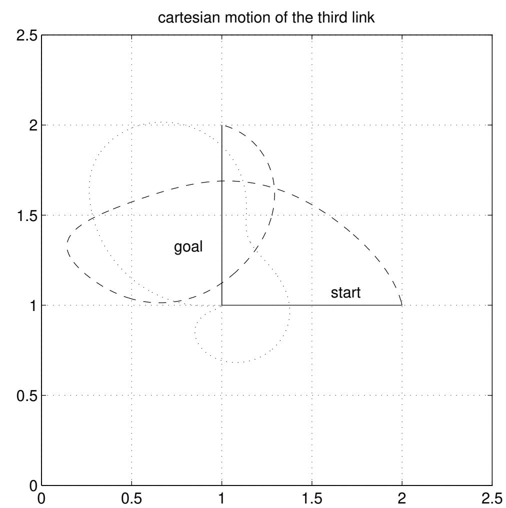

Figure 7: Motion-to-rest planning: Third link motion

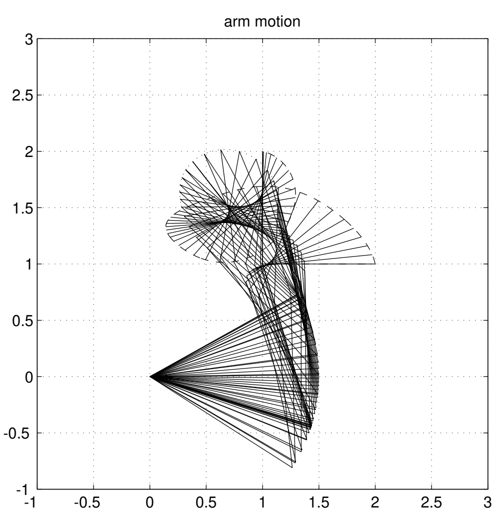

Figure 8: Motion-to-rest planning: 3R arm motion

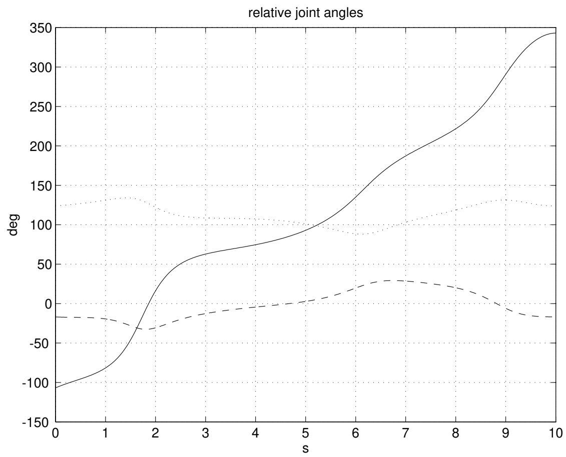

Figure 9: Motion-to-rest planning: θ_1 $(\cdots)$, θ_2 $(--)$ and θ_3 (—)

5 Trajectory tracking control

The design of a linear trajectory tracking controller is performed on the equivalent system (13). Given a desired smooth trajectory $(y_{1d}(t), y_{2d}(t))$ for the CP (planned as in Sect. 4 or with any other method), we choose

$$v_i = y_{id}^{[4]} + F_i \begin{bmatrix} y_{id}^{[3]} - y_i^{[3]} \\ \ddot{y}_{id} - \ddot{y}_i \\ \dot{y}_{id} - \dot{y}_i \\ y_{id} - y_i \end{bmatrix}, \qquad i = 1, 2, \qquad (14)$$

where the gain matrices $F_i = [\, f_{i3} \quad f_{i2} \quad f_{i1} \quad f_{i0} \,]$ assign arbitrary poles in the left-half of the complex plane to the tracking error systems. The actual states $(y_1, y_2, \ldots, y_1^{[3]}, y_2^{[3]})$ in eq. (14) are computed on-line from the measured joint positions and velocities using forward kinematics and transformations (4–5), (8) and (11).

We have simulated the tracking of the rest-to-rest trajectory of the previous section, starting from the off-path configuration: $x(0) = 0.5$ m, $y(0) = 0.9$ m, $\theta(0) = 15°$ (with zero initial velocity). The poles were all set in -2, yielding gains

$$F_1 = F_2 = [\, 8 \quad 24 \quad 32 \quad 16 \,].$$

The actual motion of the third link is shown in Fig. 10 (to be compared with Fig. 2). The evolution of the CP position errors $e_i = y_{id} - y_i$ $(i = 1, 2)$ has the prescribed exponential rate of decay. Figures 11 and 12 indicate the corresponding fast transient error for the 3R robot joint variables, with limited additional torque required with respect to the nominal case.

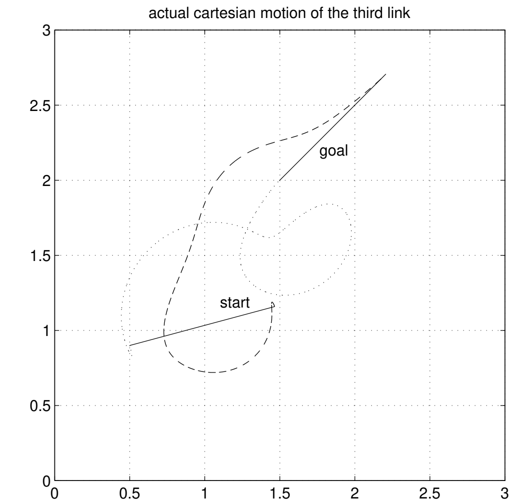

Figure 10: Trajectory tracking: Actual cartesian motion of the third link

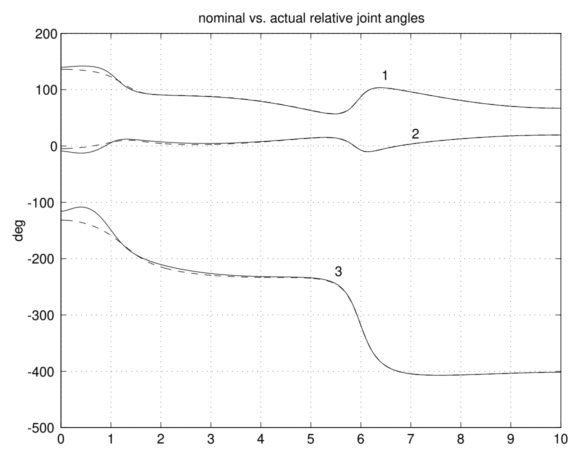

Figure 11: Trajectory tracking: Actual vs. nominal joint variables

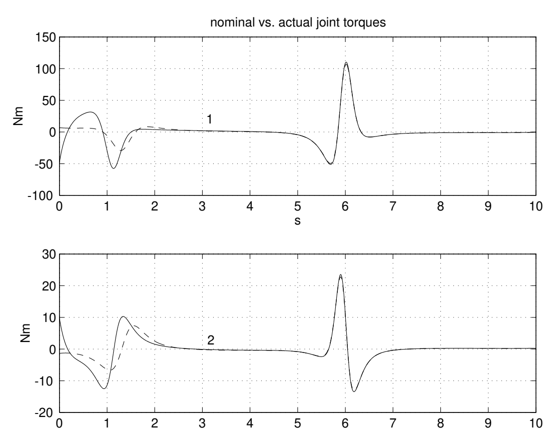

Figure 12: Trajectory tracking: Actual vs. nominal joint torques

6 Conclusions

A new method has been presented for motion planning and feedback control of the class of three-link planar robots with a passive rotational third joint. The position of the center of percussion of the third link is the linearizing output for an inversion-based control scheme based on dynamic feedback linearization. On the linear side of the problem, the design of feasible trajectories and of an exponentially stabilizing feedback is easily performed.

A comparison with [10], suggests the following remarks: *i)* the motion planner of Arai *et al.* prescribes pure translation or rotation maneuvers, while our scheme usually produces swinging motions of the third link; *ii)* the linearization procedure in this paper introduces a control singularity, which however can be avoided using the dynamic compensator state as a degree of freedom in the design; *iii)* with our method, a one-shot trajectory can be planned and a single feedback controller works throughout the motion, while multiple (up to five) motion phases with intermediate stops and controller switchings are required in [10].

The present work can be improved along several directions. A remarkable benefit can be obtained by separating path synthesis from timing law generation. In any case, other interpolating functions (polynomials of lower order, sinusoidal functions) can be used for motion planning, exploiting the arbitrary reset of the compensator states ξ and η in order to realize — without control singularities — motions with discontinuous higher-order derivatives. Finally, our preliminary results show that inclusion of gravity in the considered underactuated mechanisms is also possible within the dynamic linearization approach.

References

[1] M. W. Spong, "Underactuated Mechanical Systems," in *Control Problems in Robotics and Automation*, B. Siciliano and K. P. Valavanis Eds., LNCIS, vol. 230, pp. 135–150, Springer Verlag, London, 1998.

[2] G. Oriolo and Y. Nakamura, "Control of mechanical systems with second-order nonholonomic constraints: Underactuated manipulators," *30th IEEE Conf. on Decision and Control*, pp. 2398–2403, 1991.

[3] M. Rathinam and R. M. Murray, "Configuration flatness of Lagrangian systems underactuated by one control," *35th IEEE Conf. on Decision and Control*, pp. 1688–1693, 1996.

[4] M. W. Spong, "The swing up control problem for the Acrobot," *IEEE Control Systems*, vol. 15, no. 1, pp. 49–55, 1995.

[5] A. De Luca and G. Oriolo, "Stabilization of the Acrobot via iterative state steering," *1998 IEEE Int. Conf. on Robotics and Automation*, pp. 3581–3587, 1998.

[6] M. W. Spong and D. Block, "The Pendubot: A mechatronic system for control research and education," *34th IEEE Conf. on Decision and Control*, pp. 555–557, 1995.

[7] Y. Nakamura, T. Suzuki, and M. Koinuma "Nonlinear behavior and control of nonholonomic free-joint manipulator," *IEEE Trans. on Robotics and Automation*, vol. 13, no. 6, pp. 853–862, 1997.

[8] A. De Luca, R. Mattone, and G. Oriolo, "Stabilization of underactuated robots: Theory and experiments for a planar 2R manipulator," *1997 IEEE Int. Conf. on Robotics and Automation*, pp. 3274–3280, 1997.

[9] H. Arai, K. Tanie, and N. Shiroma, "Time-scaling control of an underactuated manipulator," *1998 IEEE Int. Conf. on Robotics and Automation*, pp. 2619–2626, 1998.

[10] H. Arai, K. Tanie, and N. Shiroma, "Nonholonomic control of a three-dof planar underactuated manipulator," *IEEE Trans. on Robotics and Automation*, vol. 14, no. 5, pp. 681–695, 1998.

[11] *Robot Motion Planning and Control*, J.-P. Laumond Ed., LNCIS, vol. 229, Springer Verlag, London, 1998.

[12] K. M. Lynch and M. T. Mason, "Stable pushing: Mechanics, controllability, and planning," *Int. J. of Robotics Research*, vol. 15, no. 6, pp. 533–556, 1996.

[13] J. Imura, K. Kobayashi, and T. Yoshikawa, "Nonholonomic control of a three-link planar manipulator with a free joint," *35th IEEE Conf. on Decision and Control*, pp. 1435–1436, 1996.

[14] A. Isidori, *Nonlinear Control Systems*, 3rd Edition, Springer-Verlag, 1995.